

**DEUTSCHES ELEKTRONEN – SYNCHROTRON**

DESY 90-163  
December 1990



**Length of Calorimeter and Effect of Absorbers in  
Front of Calorimeters**

**J. Krüger**

*II. Institut für Experimentalphysik, Universität Hamburg*

ISSN 0418-9833

**NOTKESTRASSE 85 · D-2000 HAMBURG 52**

DESY behält sich alle Rechte für den Fall der Schutzrechtserteilung und für die wirtschaftliche Verwertung der in diesem Bericht enthaltenen Informationen vor.

DESY reserves all rights for commercial use of information included in this report, especially in case of filing application for or grant of patents.

To be sure that your preprints are promptly included in the  
HIGH ENERGY PHYSICS INDEX,  
send them to the following address (if possible by air mail):

DESY  
Bibliothek  
Notkestrasse 85  
2 Hamburg 52  
Germany

DESY 90 - 163  
December 1990

LENGTH OF CALORIMETERS  
AND  
EFFECT OF ABSORBERS IN FRONT OF CALORIMETERS \*

Jürgen Krüger

II. Institute for Experimental Physics, Hamburg University,  
Luruper Chaussee 149, D-2000 Hamburg 50, Germany

for the ZEUS Calorimeter Group

ABSTRACT

A detailed analysis of the longitudinal hadron shower development was performed with the longitudinally finely segmented WA78 calorimeter at CERN (5-210GeV). The shower containment studies allow an optimization of the depth of hadron calorimeters and a reasonable extrapolation for particles and jets to very high energies ( $\approx 1\text{TeV}$ ).

The effect of material in front of calorimeters for hadrons, electrons and jets was studied systematically with the ZEUS forward calorimeter prototype at CERN at energies from 0.5 to 100GeV.

\* Talk given at the ECFA Large Hadron Collider Workshop, Aachen,  
4 - 9 October 1990

# 1. LENGTH OF CALORIMETERS

## 1.1 INTRODUCTION

The optimum length of a hadron calorimeter is directly related to the longitudinal development of hadron showers.

Longitudinal shower profiles have been measured for single particles and jets with the WA78 hadron calorimeter at CERN in the energy range from 5GeV to 210GeV [1],[2].

A detailed analysis of shower containment and the influence of dead material (e.g. PM-boxes) inside the calorimeter was performed in particular with respect to the optimization of the depth of the high resolution ZEUS uranium scintillator calorimeter ( $\sigma_h/E \approx 35\%/\sqrt{E}$ ) and extrapolations to higher energies are performed.

## 1.2 THE WA78-H1-ZEUS CALORIMETER TEST

The WA78 hadron calorimeter (Fig. 1) consists of two parts with different absorber material, upstream uranium layers ( $60 \times 60 \times 1 \text{ cm}^3$ ) and downstream iron layers ( $60 \times 60 \times 2.5 \text{ cm}^3$ ). The 1st part ( $5.4\lambda$ ) was operated with 12 modules of depleted uranium (10mm)/scintillator (5mm), 4 elements per module ( $0.45\lambda$ ) and the 2nd part ( $8\lambda$ ) with 13 modules of iron (25mm)/scintillator (5mm), also 4 elements per module ( $0.62\lambda$ ).

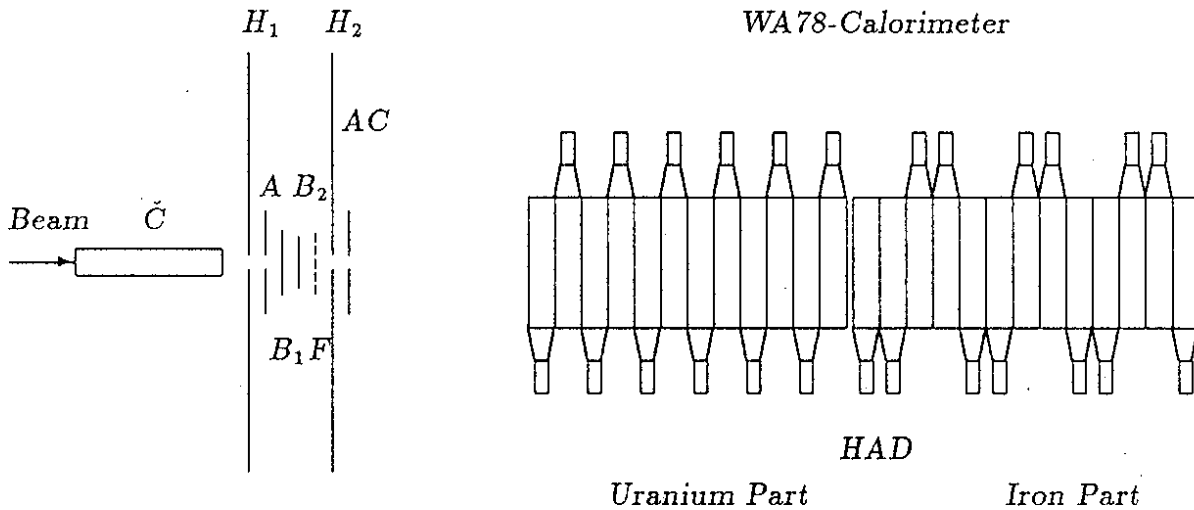


Fig. 1 The Experimental Set-Up of the WA78-H1-ZEUS Test

## 1.3 LONGITUDINAL HADRON SHOWER DEVELOPMENT AND SHOWER CONTAINMENT

The WA78 calorimeter has the advantage of a fine longitudinal readout segmentation ( $0.45\lambda$ ). Data have been taken from 5GeV to 210GeV and thus allow an extrapolation to higher energies.

Figure 2 shows the longitudinal hadron shower profiles from 5 to 210GeV for all hadrons ( $\equiv$  single hadrons) as function of the calorimeter depth in units of nominal interaction lengths  $\lambda$ . Figure 3 is similar to Fig. 2, but for events with shower vertices in the first module ( $0.45\lambda$ ) of the calorimeter. These events are considered to behave like jet-like objects and are also called jets in the following.

There are some limitations of the data in particular at high energy (135GeV/210GeV), where the PMs have been run at reduced gain, due to pedestal problems and transverse shower containment.

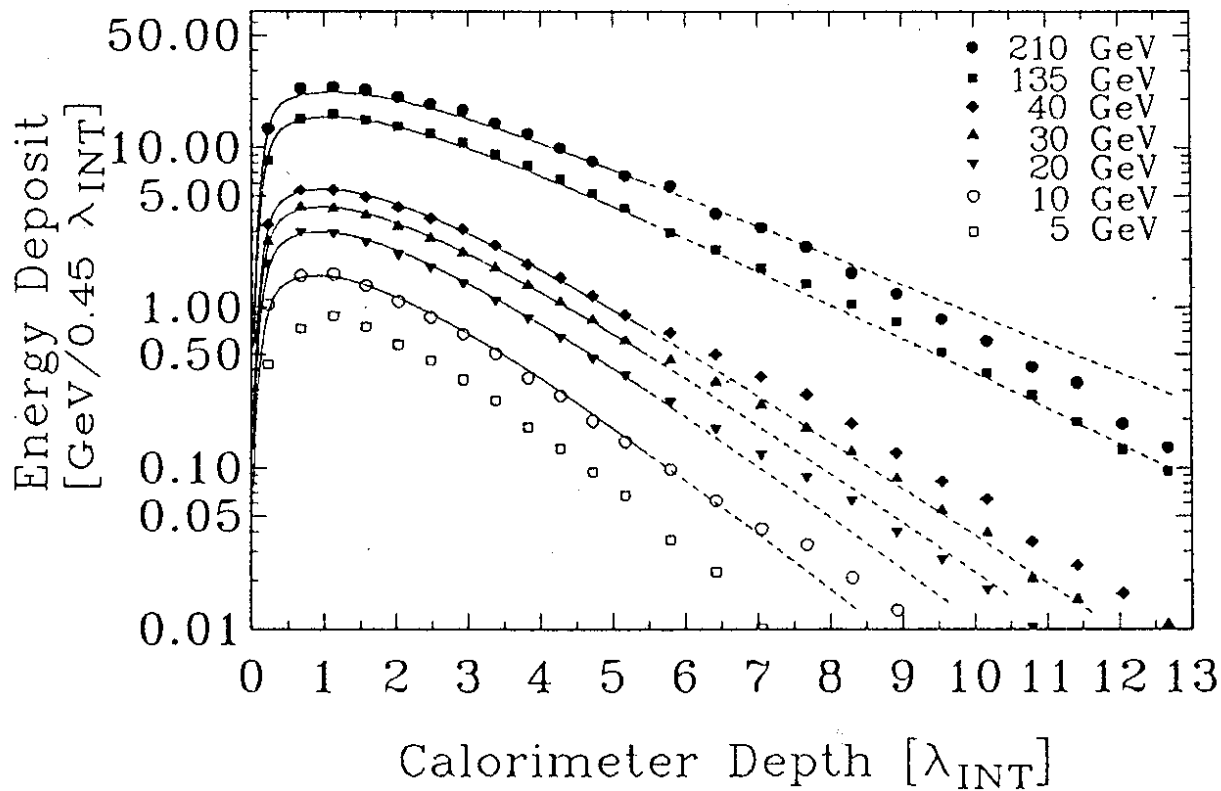


Fig. 2 Longitudinal Shower Profiles for Beam Momenta of 5 to 210 GeV for all Events

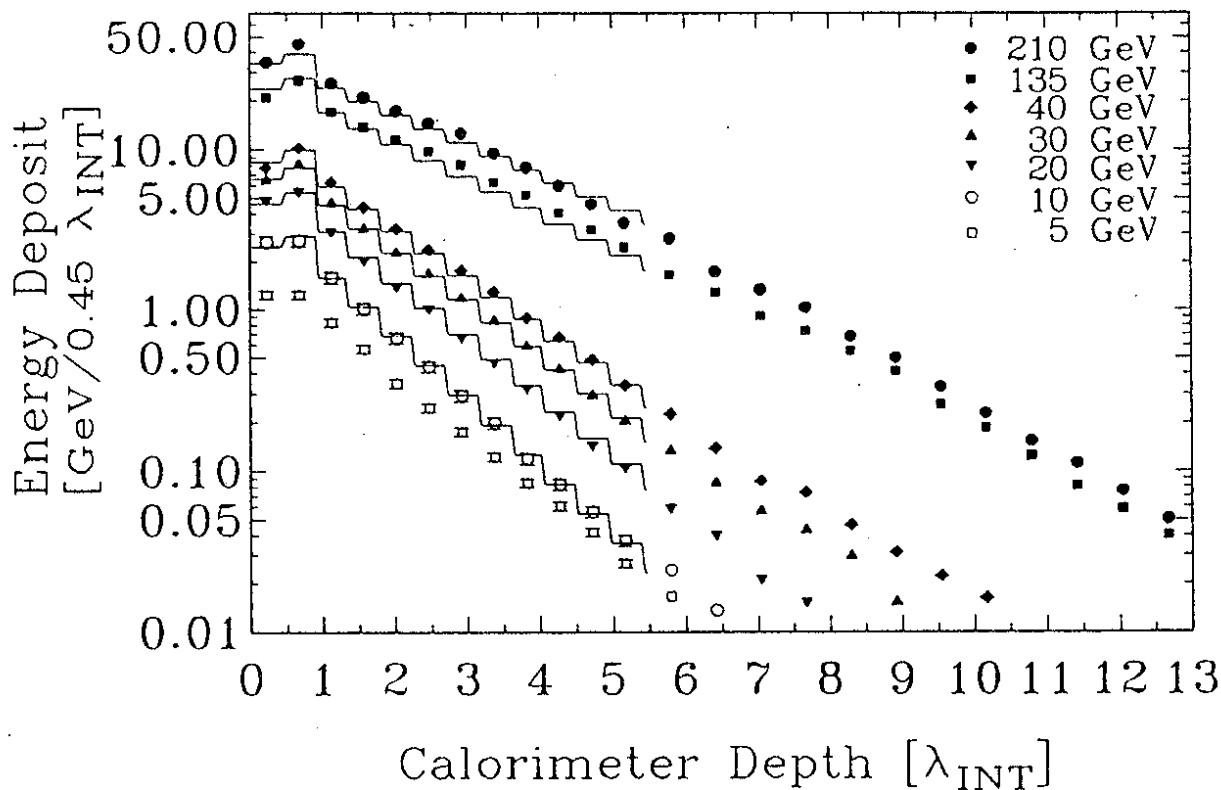


Fig. 3 Longitudinal Shower Profiles for Beam Momenta of 5 to 210 GeV for Events with Shower Vertices in the First Module

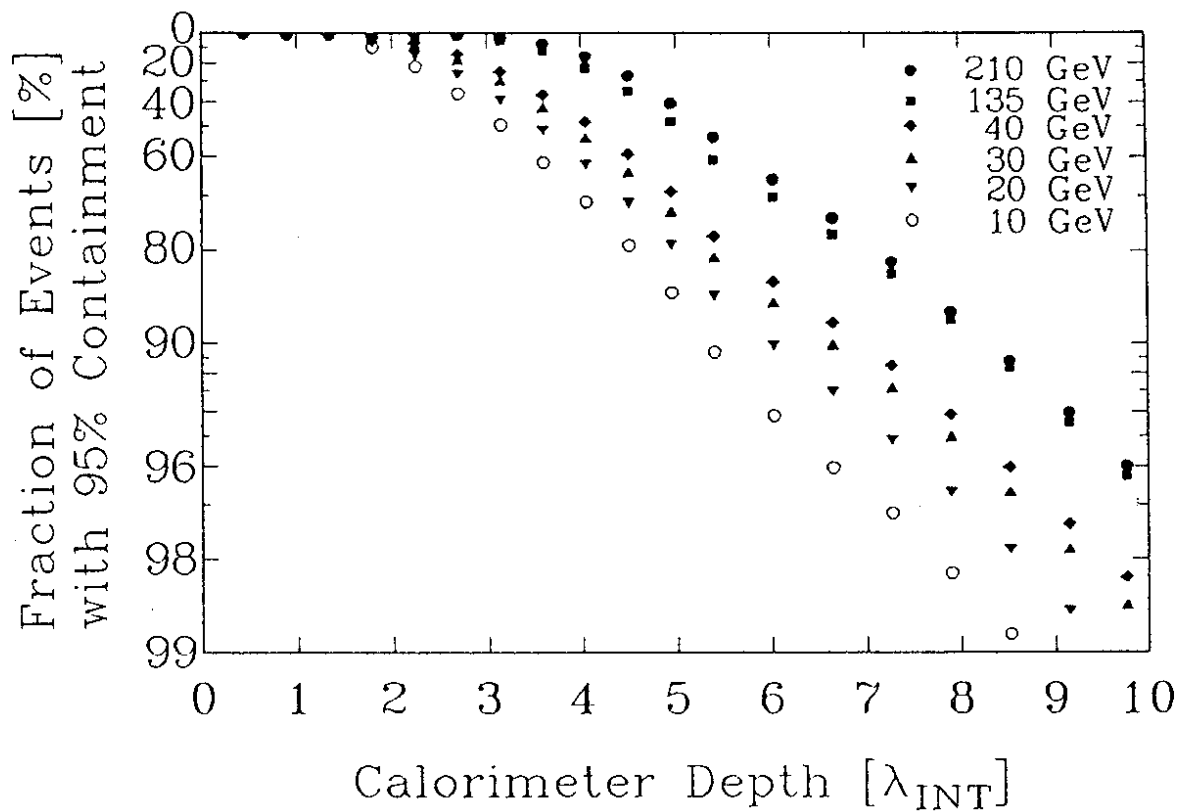


Fig. 4 Fraction of Events with 95% Energy Containment as a Function of the Calorimeter Depth for all Hadrons

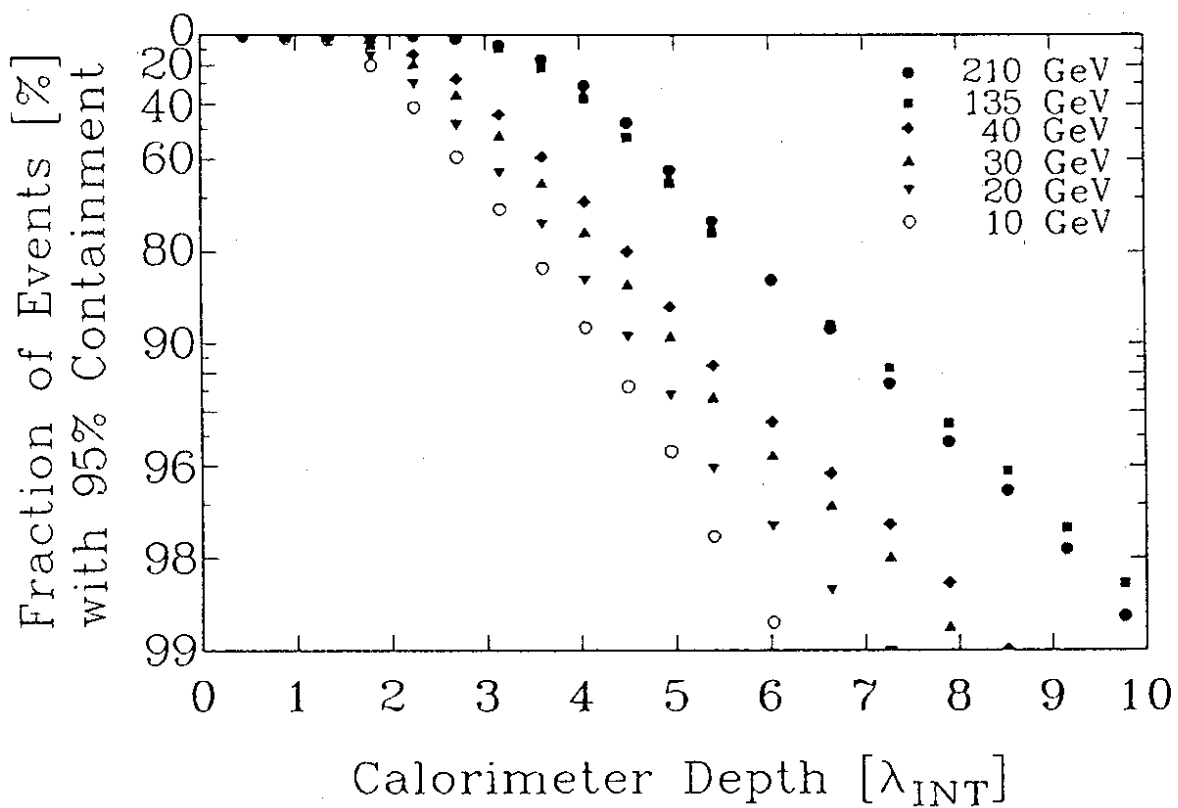


Fig. 5 Fraction of Events with 95% Energy Containment as a Function of the Calorimeter Depth for Events with Shower Vertices in the First Module

A phenomenological function has been fitted to the data. The parametrization of the energy deposit  $dE/dx(x)$  (Fig. 3) as a function of the distance  $x$  in interaction lengths from the shower vertex is:

$$\frac{dE}{dx}(x) = E_0 \left\{ \alpha \frac{b^{a+1}}{\Gamma(a+1)} x^a \exp(-bx) + (1-\alpha) c \exp(-cx) \right\}$$

where  $E_0$  is the incident energy,  $a=3$ ,  $b[\lambda^{-1}]=19.5$ ,  $\alpha=0.13\pm 0.02$  and  $c[\lambda^{-1}]=(0.67\pm 0.03)-(0.166\pm 0.003) \ln(E_0[\text{GeV}]/50)$ . The function describes well the data for energies above 10 GeV (see Fig. 2, 3).

The shower distributions measured from the front end of the calorimeter ( $t$ ) for all hadrons are given by the convolution of  $dE/dx(x)$  with the position of the first shower vertices:

$$\frac{dE}{dt} = \frac{1}{\lambda_\pi} \int_0^t \exp\left(-\frac{x}{\lambda_\pi}\right) \frac{dE}{dx}(t-x) dx$$

where  $\lambda_\pi = 1.11$  represents the interaction length of the incoming hadrons.

In order to determine the optimum length of a calorimeter the fraction of events with a certain shower containment has to be known. The fractions of all hadrons and jets with a shower containment of 95% in the calorimeter as function of the calorimeter depth are presented in Fig. 4 and 5. The criterium for the depth of the ZEUS calorimeter was for example that 90% of the jets of the maximum energy allowed by kinematics are contained in the uranium scintillator calorimeter with 95% of their energy [3]. This high resolution calorimeter is followed by a coarser backing calorimeter of 4 - 6  $\lambda$  depth.

#### 1.4 LEAKAGE DUE TO DEAD AREAS

The data offers also the possibility to investigate the influence of dead material, such as PM boxes, at various places inside the calorimeter [1].

The influence on the resolution due to the shower energy lost in the dead material of  $0.6\lambda$  behind  $5.4\lambda$  has been studied for 40 GeV jets (start vertex of showers in the 1st module ( $0.45\lambda$ )) and behind  $7.2\lambda$  for 135 GeV jets. The information of the longitudinally finely segmented WA78 calorimeter has been combined to a calorimeter configuration as presented in Fig. 6 that corresponds to the ZEUS calorimeter system. It consists of a high resolution hadron calorimeter (a) plus veto readout section (necessary only for higher energies) (b), dead material (PM boxes, iron shielding) (c) and a coarser backing calorimeter (d).

The fraction of events contributing to a nongaussian tail due to the energy lost in the dead material (PM boxes) is measured in units of the calorimeter resolution for hadrons ( $\sigma_h/E=35\%/\sqrt{E} \equiv \sigma_{35}$ ) as function of the calorimeter depth. This is shown for jets in Fig. 7 and in Fig. 8 for the additional requirement that less than 2% of the shower energy are deposited in the backing calorimeter ( $E_{BAC} < 2\%$ , valid for about 90% of the events).

With a calorimeter depth of  $5.4\lambda$  about 2.6% of 40 GeV jets are found additionally outside  $1\sigma_{35}$  and 0.6% outside  $2\sigma_{35}$ .

A corresponding investigation with a calorimeter depth of  $7.2\lambda$  and 135 GeV jets shows that about 3% are additionally outside  $1\sigma_{35}$  and 0.6% outside  $2\sigma_{35}$ .

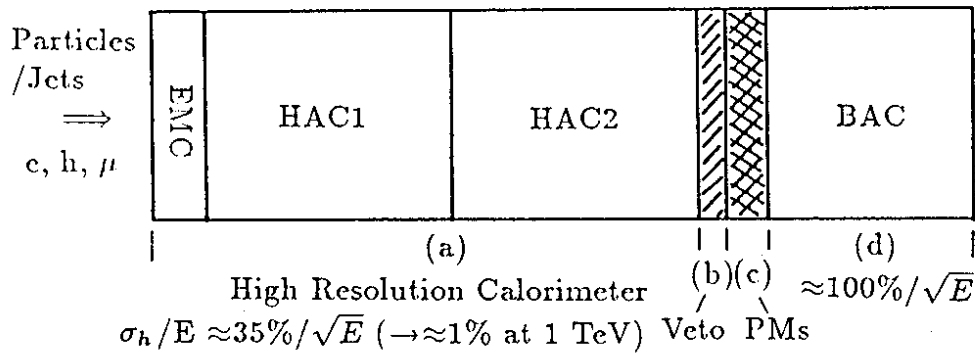


Fig. 6 Calorimeter Design of a High Resolution Calorimeter (a), (Veto Readout Section (b),) PM Boxes (c) and Backing Calorimeter (d)

Jets additionally outside  $i\sigma_{35}$

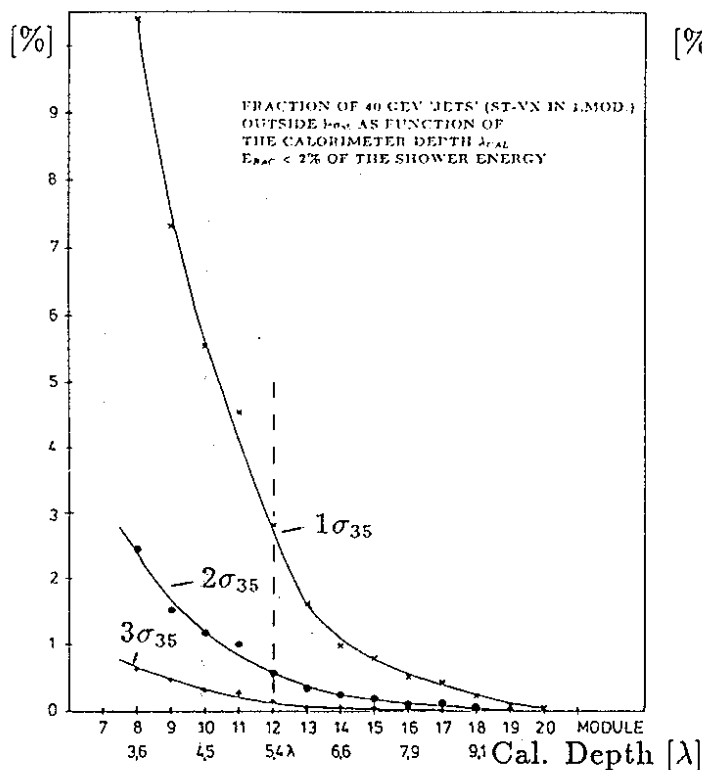


Fig. 7 Fraction of 40 GeV 'Jets' outside  $i\sigma_{35}$  as Fct. of the Calorimeter Depth and  $E_{BAC} < 2\%$  of the Shower Energy

Jets additionally outside  $i\sigma_{35}$

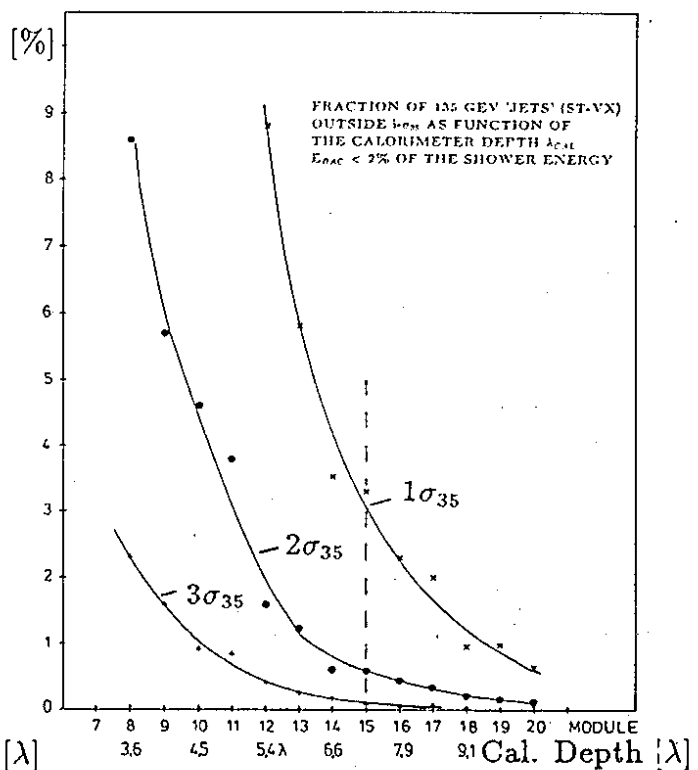


Fig. 8 Fraction of 135 GeV 'Jets' outside  $i\sigma_{35}$  as Fct. of the Calorimeter Depth and  $E_{BAC} < 2\%$  of the Shower Energy

### 1.5 EXTRAPOLATION TO 1 TEV PARTICLES AND JETS

As already mentioned a reasonable extrapolation to higher energies is also possible with these data [4].

The calorimeter depth needed for a certain shower containment (90%, 92.5%, 95%, 97.5%) as function of the energy for 90% of single hadrons is presented in Fig. 9 and for 90% of jets in Fig. 10. An extrapolation to 1 TeV is also indicated.

The study of the calorimeter depth has been done with uranium (/iron) and uranium calorimeters. For other materials (Al and Pb) the necessary depths in units of  $\lambda$  may differ somewhat.



Cal. Depth

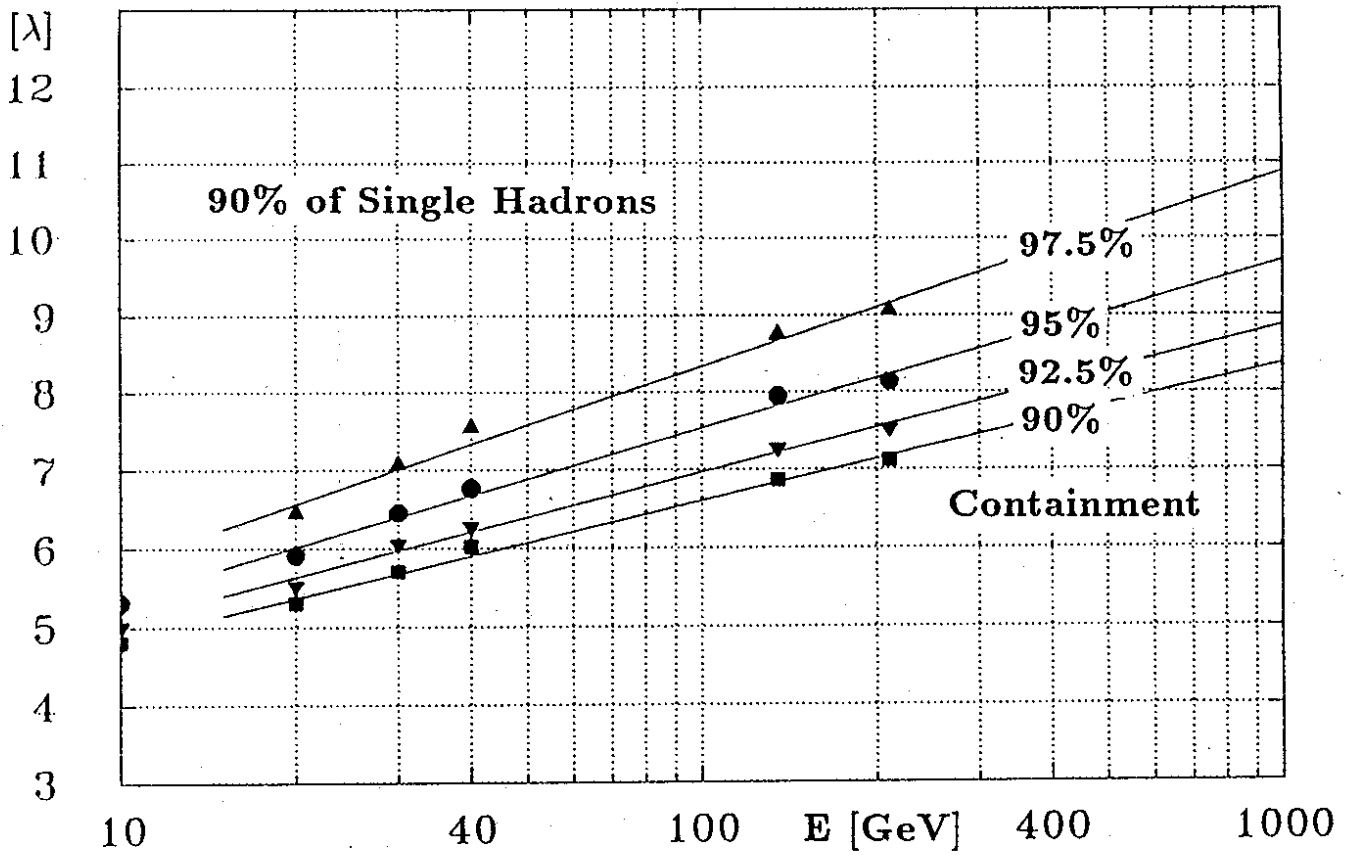


Fig. 9 Calorimeter Depth required for Different Fractions of Shower Containment for 90% of Single Hadrons as Function of the Energy

Cal. Depth

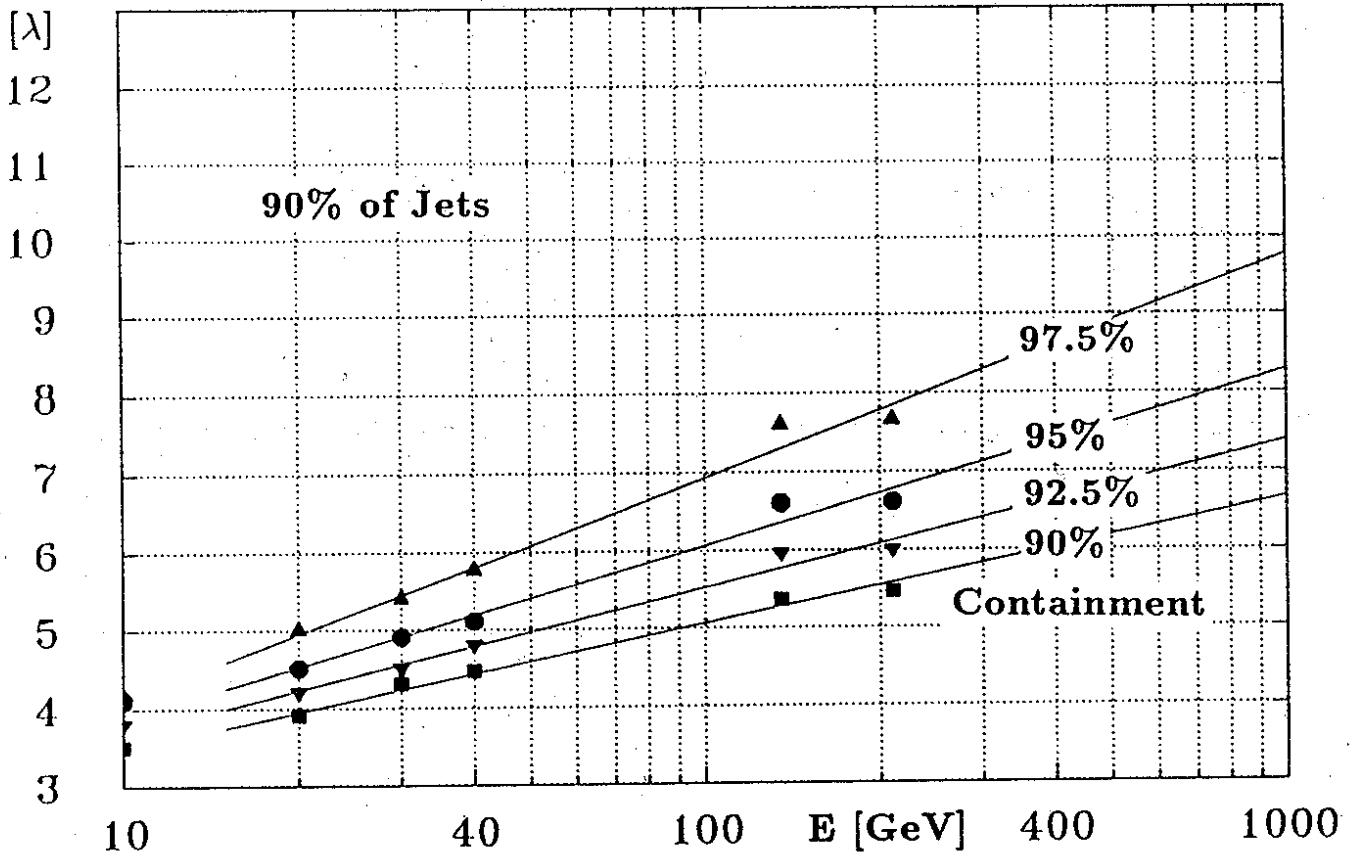


Fig. 10 Calorimeter Depth required for Different Fractions of Shower Containment for 90% of 'Jets' as Function of the Energy

Cal. Depth

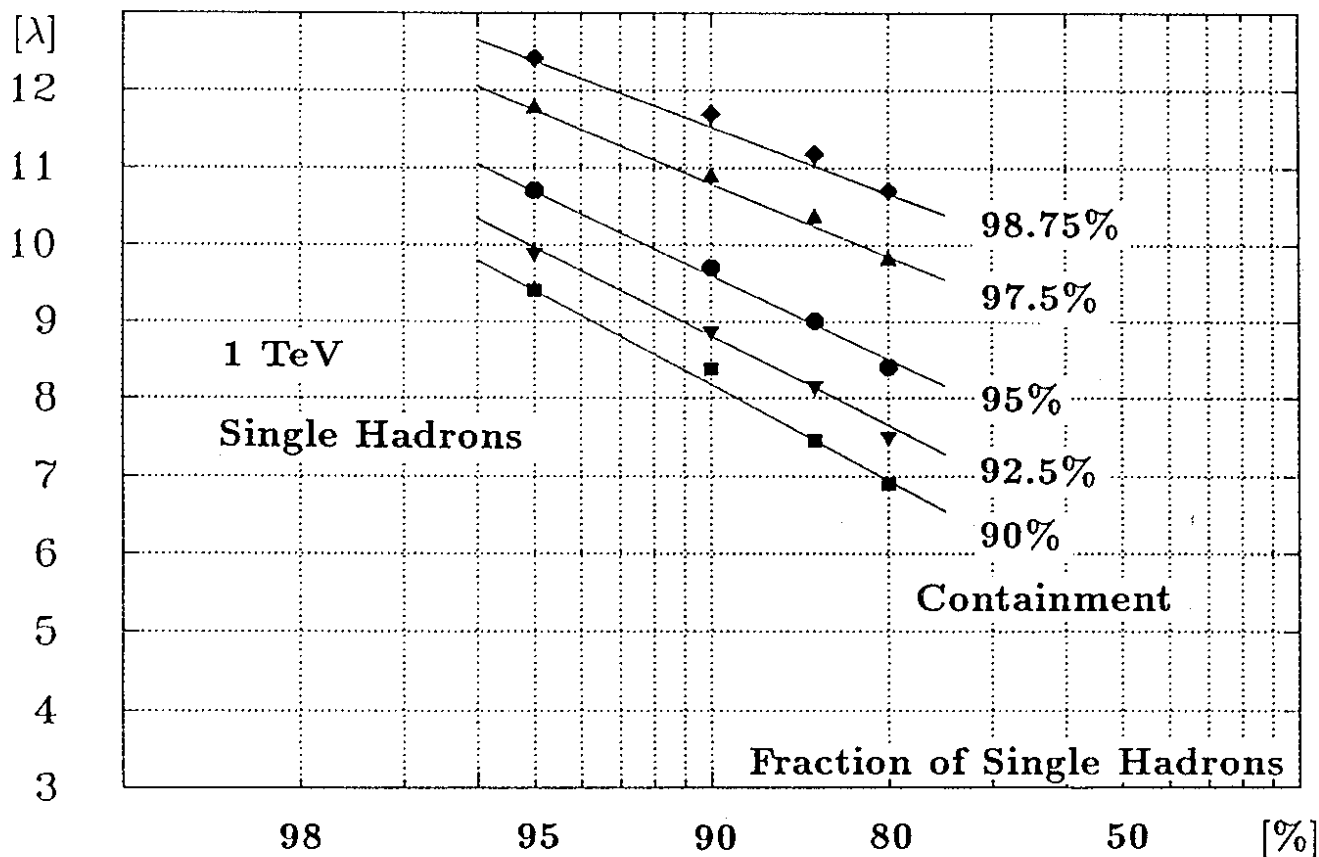


Fig. 11 Calorimeter Depth required for Different Fractions of Shower Containment for 1 TeV Single Hadrons [Extrapol.] as Fct. of the Fraction of Single Hadrons

Cal. Depth

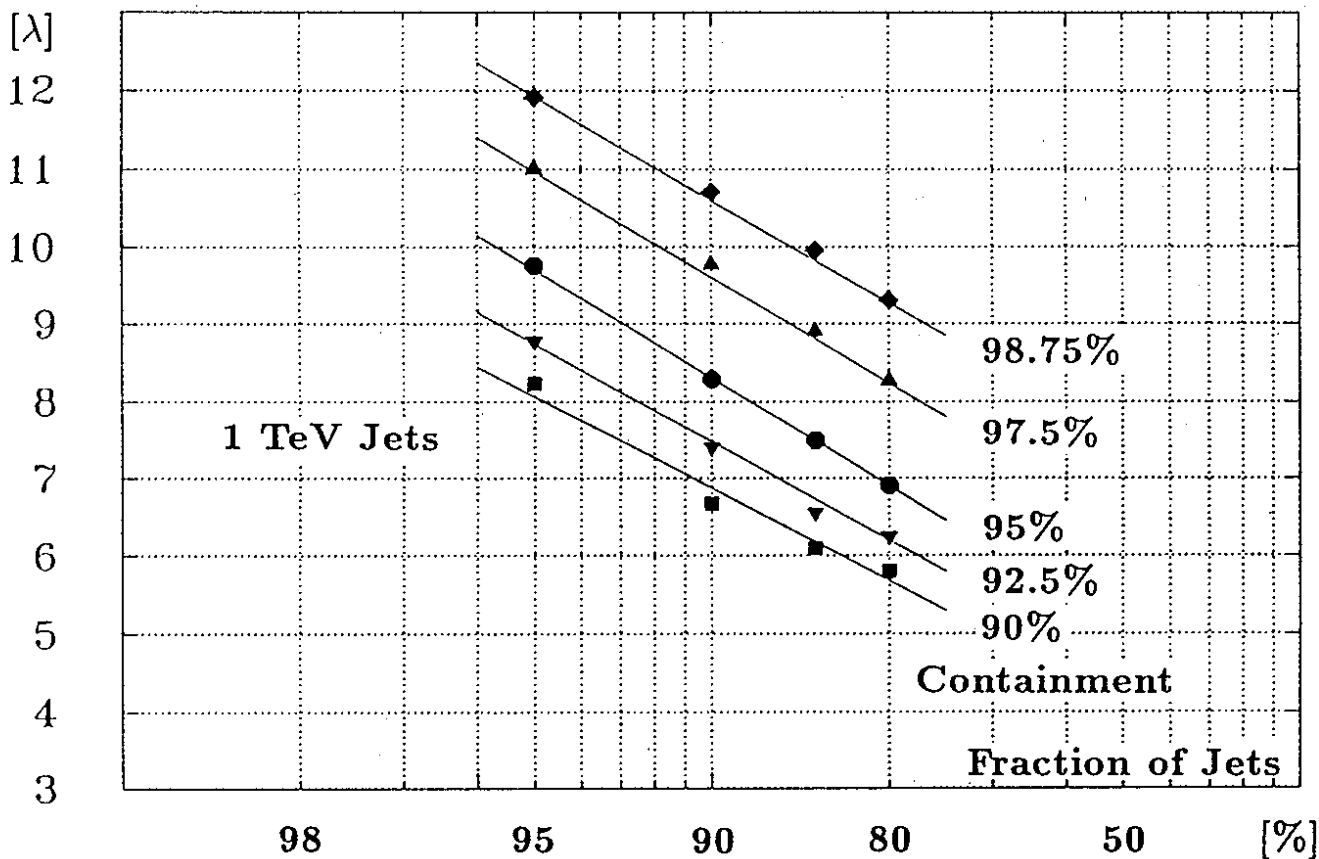


Fig. 12 Calorimeter Depth required for Different Fractions of Shower Containment for 1 TeV 'Jets' [Extrapolation] as Function of the Fraction of 'Jets'

Figure 11 and 12 show the calorimeter depth necessary for 1 TeV single hadrons and jets (extrapolations) with a certain shower containment as function of the fraction of single hadrons and jets.

For 85% - 90% of the 1 TeV jets with a shower containment of 98.75% a calorimeter depth of about  $10\lambda - 10.5\lambda$  is needed. This is equivalent to about 95% of the 1 TeV jets having a shower containment of 95% at  $9.5\lambda - 10\lambda$ .

At 1 TeV the energy resolution of a high resolution hadron calorimeter with  $\sigma_h/E \approx 35\%/\sqrt{E}$  approaches 1%. In order not to lose this excellent energy resolution at very high energies due to energy lost in the dead material of the PM boxes a very promising solution is to install an additional readout section in front of the dead material as veto counter to select events fully contained in the high resolution calorimeter as indicated in Fig. 6.

## 2. EFFECT OF ABSORBERS IN FRONT OF CALORIMETERS

### 2.1 INTRODUCTION

Very often tracking chambers, a magnet coil and various mechanical constructions are installed in front of a calorimeter. For example the material in front of the high resolution ZEUS uranium scintillator calorimeter is over a wide range about 1-1.5 radiation lengths  $X_0$ . But there are also narrow peaks up to  $4 X_0$  at a few small regions where mechanical support structures are necessary. This material degrades the measured signal and the energy resolution of the calorimeter.

### 2.2 MEASUREMENT PROGRAM WITH THE FCAL PROTOTYPE

Systematic measurements with various thicknesses of absorber (Al) directly in front of the ZEUS forward calorimeter (FCAL) prototype [5] have been performed at CERN in the momentum range from 0.5 to 100 GeV/c to determine quantitatively the effect of absorbers [6], [4].

The FCAL prototype (Fig. 13) consists of four modules with a front area of 80cm x 80cm ( $4 \times (20\text{cm} \times 80\text{cm})$ ), a depth of 2m ( $7\lambda$ ) and 192 PMs [5], [7].

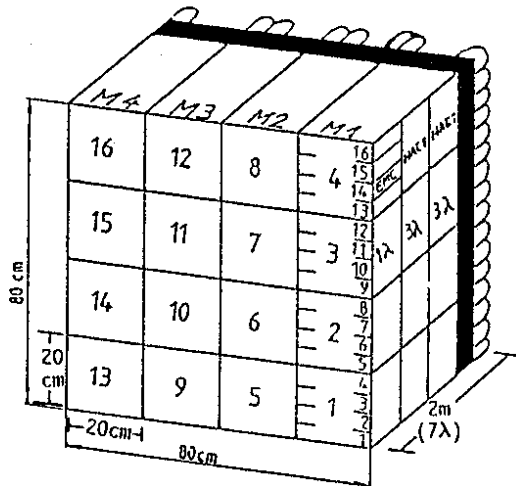


Fig. 13 The Module, Tower and Longitudinal Structure of the FCAL Prototype

The experimental set up used at CERN consisted of the scintillation beam counters B1, B2, B3 and B4 defining the beam, two Cherenkov counters C1 and C2 and the FCAL prototype calorimeter itself (Fig. 14).

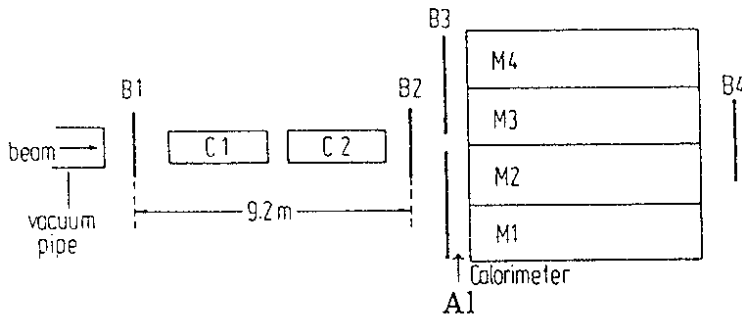


Fig. 14 The Experimental Set-Up with the FCAL Prototype at CERN

Without material in front of the prototype the energy resolution is  $\sigma_h/E=35\%/\sqrt{E}$  for hadrons and  $\sigma_e/E=18\%/\sqrt{E}$  for electrons and above 3GeV the ratio of electron to hadron response  $e/h$  is about 1 [5].

The main points of the measurement program are listed in the following:

Hadrons and Electrons

Absorber: Aluminium Thickness: 0cm, 9cm, 18cm, 27cm (= 0, 1, 2, 3  $X_0$ )  
Momentum: at CERN PS: 0.5, 1, 2, 3, 5 GeV/c  
at CERN SPS: 10, 20, 30, 75 GeV/c

Hadrons and Interaction Trigger - Jets

Absorber: Aluminium Thickness: 0cm, 4cm, 10cm  
Momentum: at CERN SPS: 50, 100 GeV/c

### 2.3 EXPERIMENTAL RESULTS

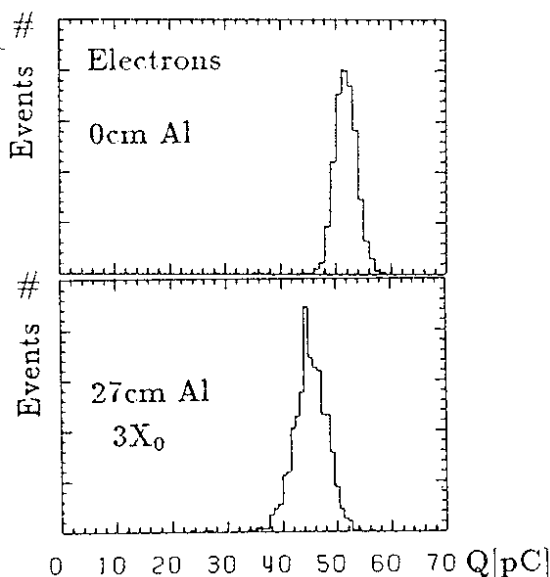


Fig. 15 Pulse Height Spectra for 30GeV Electrons without and with 27cm Al in Front of the Calorimeter

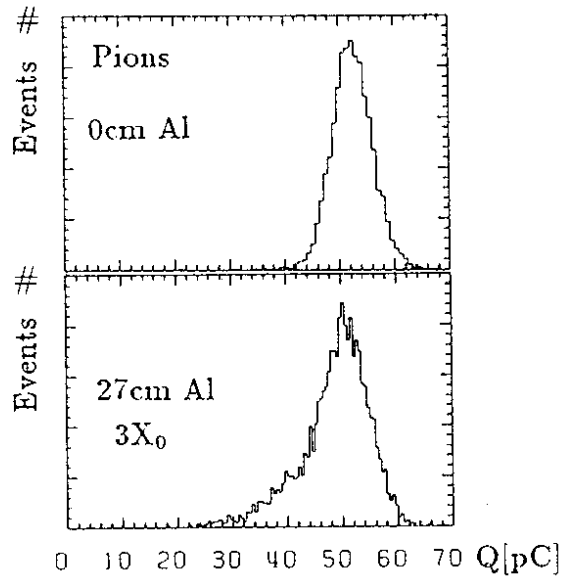


Fig. 16 Pulse Height Spectra for 30GeV Pions without and with 27cm Al in Front of the Calorimeter

Figure 15 and 16 show the pulse height spectra for electrons and pions at 30GeV without and with 27cm Aluminium absorber ( $3X_0$ ) directly in front of the prototype. With absorber in front the mean values of the spectra are shifted significantly to lower values and the widths of the distributions increase. Whereas for electrons the shape remains approximately Gaussian, it becomes strongly asymmetric for hadrons with a tail to small pulse heights.

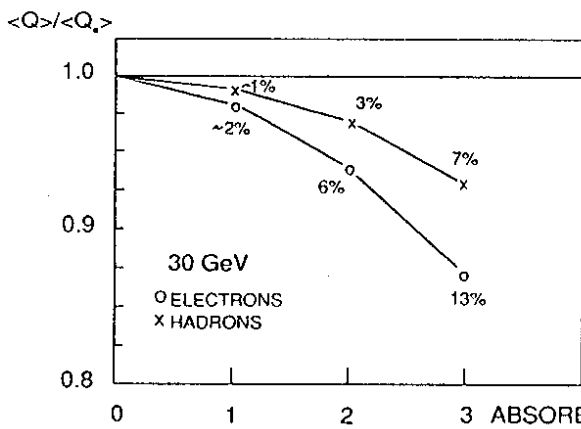


Fig. 17 Ratio of the Mean Signal Height with Absorber ( $\langle Q \rangle$ ) and without Absorber ( $\langle Q_0 \rangle$ ) as Function of the Absorber Thickness

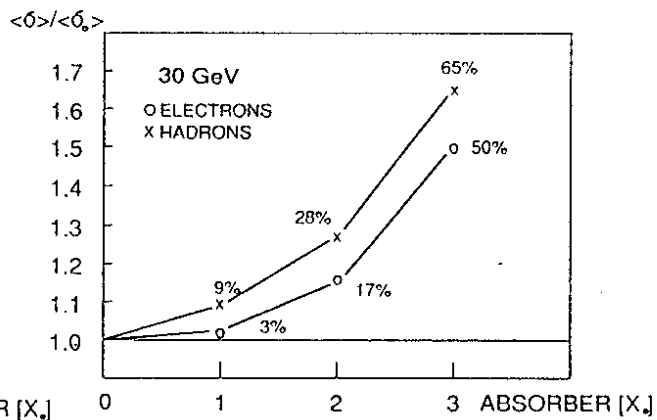


Fig. 18 Ratio of the Standard Deviation with Absorber ( $\langle \sigma \rangle$ ) and without Absorber ( $\langle \sigma_0 \rangle$ ) as Function of the Absorber Thickness

Figure 17 and 18 show for electrons and hadrons at 30 GeV the ratio of the mean signal height and the standard deviation ( $3\sigma$  cut used) with material ( $\langle Q \rangle$ ,  $\langle \sigma \rangle$ ) and without material ( $\langle Q_0 \rangle$ ,  $\langle \sigma_0 \rangle$ ) as function of the absorber thickness in front of the calorimeter. For 1  $X_0$  material in front the mean value is reduced by about 1% for hadrons and 2% for electrons and decreases significantly in particular for electrons with increasing absorber thickness. The widths increase with absorber material in front and are for 1  $X_0$  by about 3% larger for electrons and 9% larger for hadrons.

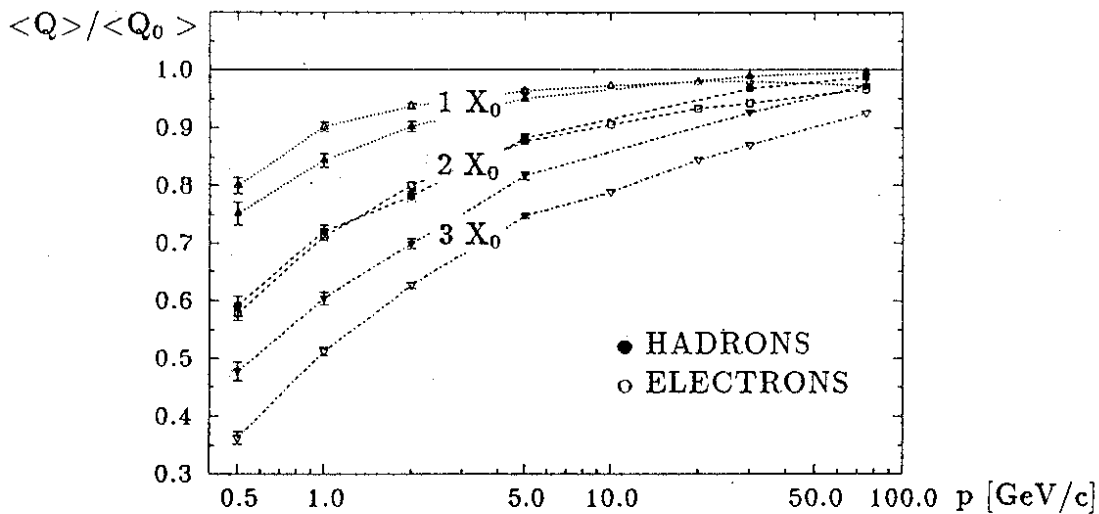


Fig. 19 Ratio of the Mean Signal Height with Absorber ( $\langle Q \rangle$ ) and without Absorber ( $\langle Q_0 \rangle$ ) as Function of the Momentum

The ratio  $\langle Q \rangle / \langle Q_0 \rangle$  for 9cm, 18cm and 27cm Aluminium absorber as function of the particle momentum is shown in Fig. 19. The deviation from 1 is large at low momenta and is decreasing with increasing momentum. Monte Carlo simulations have been performed and a similar behaviour has been found [6].

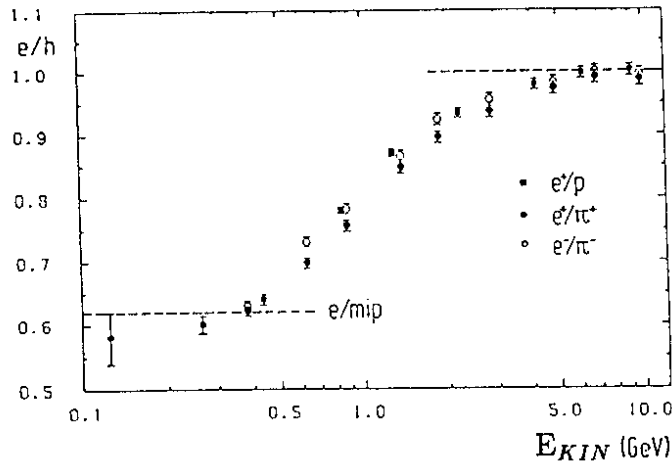


Fig. 20  $e/h$  as Function of the Kinetic Energy  $E_{KIN}$  for  $p$ ,  $\pi^+$ ,  $\pi^-$

Figure 20 shows the  $e/h$  ratios at equal kinetic energies  $E_{KIN}$  for  $\pi^+$ ,  $\pi^-$  and  $p$  [5].  $e/h$  is the same for  $\pi^+$ ,  $\pi^-$  and  $p$  and depends in first approximation only on the kinetic energy  $E_{KIN}$ , the energy available for particle production and energy deposit in the calorimeter. At low energies hadrons lose more and more of their energy via  $dE/dx$  and approach the sampling fraction of a minimum ionizing particle (mip). Thus  $e/h$  approaches  $e/mip$ , which is 0.62 in the present calorimeter. As the electron response  $e$  is essentially linear with kinetic energy, the ratio  $\langle Q \rangle / E_{KIN}$  normalized to  $\langle Q_0 \rangle / E_{KIN}$  at 75 GeV ( $(\langle Q \rangle / E_{KIN}) |_{75 GeV}$ ) with absorber in front shows smaller deviations from 1.

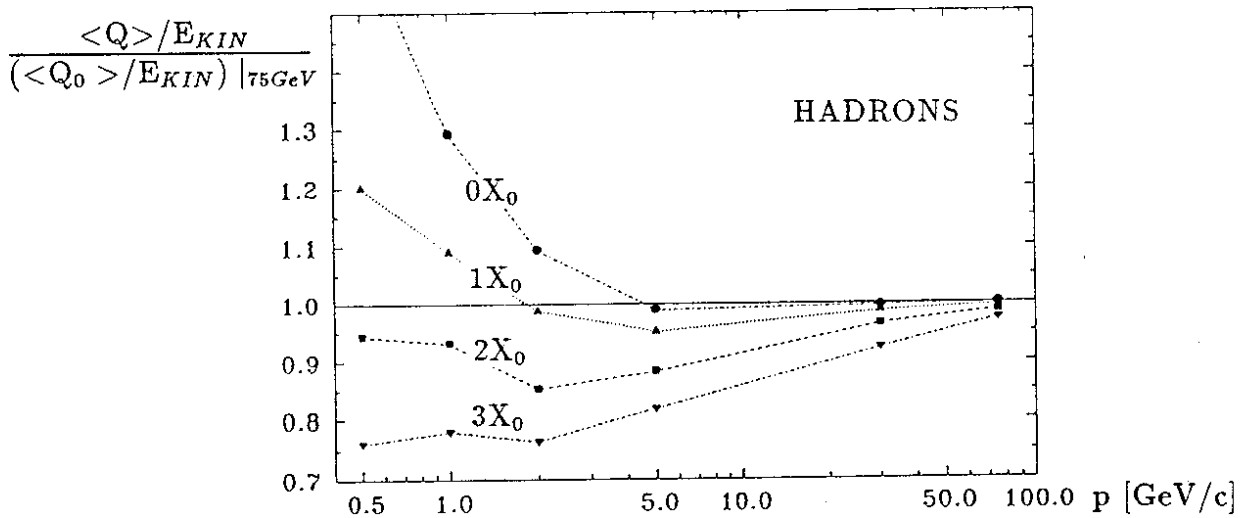


Fig. 21 Ratio of the Mean Signal Height ( $\langle Q \rangle$ ) and the Kinetic Energy  $E_{KIN}$  as Function of the Momentum

The normalized ratio  $\langle Q \rangle / E_{KIN}$  is shown in Fig. 21 for hadrons as function of the momentum. The different curves show the dependence on the absorber thickness. The deviation from 1 is significantly reduced compared to  $\langle Q \rangle / \langle Q_0 \rangle$ .

The analysis of the data taken with the interaction trigger in front of the FCAL prototype and the study of methods to correct experimentally for energy lost in the absorber in front of the calorimeter via pulse height measurement are in progress [7].

## ACKNOWLEDGEMENTS

I gratefully acknowledge the efficient cooperation of the participants of the various groups during the WA78-H1-ZEUS calorimeter test. I am also very grateful to my colleagues of the ZEUS calorimeter group for their excellent collaboration during the tests with the ZEUS FCAL prototype calorimeter. For the fruitful cooperation and numerous interesting discussions especially with respect to the ZEUS calorimeter R. Klanner, E. Lohrmann and G. Wolf are warmly acknowledged.

## REFERENCES

1. Krüger, J., "Shower Development in a Uranium/Scintillator Calorimeter (WA78) and the Requirements for the Hadron Calorimeter of the ZEUS Detector", DESY, ZEUS Note 86-019 (1986)
2. Catanese, M.G. et al., "Hadron, Electron and Muon Response of a Uranium-Scint. Calorimeter", Nucl. Instr. and Meth. A260 (1987) 43-54
3. The ZEUS Detector, Technical Proposal, DESY, March 1986  
The ZEUS Detector, Status Report 1987, DESY, September 1987  
The ZEUS Detector, Status Report 1989, DESY, March 1989  
Wolf, G., "HERA: Physics, Machine and Experiments", DESY 86-089
4. Krüger, J., "The ZEUS Uranium Scintillator Calorimeter ... ", Hamburg, DESY, in preparation
5. Behrens, U. et al., "Test of the ZEUS Forward Calorimeter Prototype", Nucl. Instr. and Meth. A289 (1990) 115  
Andresen, A. et al., "Response of a Uranium-Scintillator Calorimeter to Electrons, Pions and Protons in the Momentum Range 0.5 - 10 GeV/c", Nucl. Instr. and Meth. A290 (1990) 95
6. Fürtjes, A., Diploma Thesis, Münster (1990), DESY F35-90-02
7. Kröger, W. et al., "The Interaction Trigger ...", DESY, in preparation